

Accounts

Dendrimer Complexes Based on Fine-Controlled Metal Assembling

Kimihisa Yamamoto* and Takane Imaoka

Department of Chemistry, Faculty of Science and Technology, Keio University,
3-14-1 Hiyoshi, Kohoku-ku, Yokohama 223-8522

Received August 22, 2005; E-mail: yamamoto@chem.keio.ac.jp

A series of novel dendrimers composed of dendritic phenylazomethines (DPAs) were synthesized with several types of functional cores. The metal assembling to the DPAs is stepwise by the layers, therefore, they can be used as a scaffold for the precise hybridization between metal ions and organic macromolecules. Because of uniform structure of the dendrimer, there is no structural dispersion in the macromolecule–metal hybrid of the DPAs. Also, the number of metal ions loaded in one dendrimer should have no statistical distribution in principle due to the precise metal assembling. A rigid π-conjugating backbone structure contributes not only to the stepwise metal assembly, but also to the solid-state stability under high temperature. Development of this property without any reduction in solubility in organic media enabled the easy preparation of homogeneous amorphous films in which the metal and macromolecule are precisely hybridized. As a result, the thin solid of the metal-assembling dendrimer acts as an excellent organic semiconductor in the hole-transport layer of a light-emitting diode. Metal-assembling DPAs also enhance the electron-transfer reaction as a protein-like catalyst. The DPA having a cobalt porphyrin core-could catalyze the CO_2 reduction at an applied overpotential 1.1 V lower than that needed for the catalysis by a model compound of the porphyrin core (CoTPP). Reversible encapsulation/release of multiple irons is also demonstrated as a mimic of the iron storage protein (Ferritin). The switching between these two coordinating states can be completely controlled by the redox states of the iron (Fe^{II}/Fe^{III}). The finding of these unique dendritic ligands will afford new insight into molecular design for finely controlled macromolecule–metal hybrid materials.

1. Metallo-Dendrimer Complexes

Macromolecule–metal complexes[1] are defined as molecular-level hybrids built up with metal complexes and organic polymers. They have been noted in evolution of novel functions based on synergetic effect between the functionality of each part (metal and polymer). For example, applications of these materials for fixation of catalysts,[2] functional modified electrodes based on electron[3–5]/ion[6] conductivity, electron-spin control,[7] and amplification of photoelectron conjugating properties[8] demonstrate outstanding enhancement. Most of them are induced by (1) supporter effect, (2) concentration/dilution effect, (3) environmental effect, (4) conformational effect, and (5) cooperative/concerted effect by micro domains in the polymers. For maximum use of these domains, a general methodology that can handle the higher-order structure of the hybrids is strongly required. All the molecular, hybrid, and higher-order structures of the conventional macromolecule–metal complexes are however dispersed with statistical distribution, and impossible to fix themselves into one limited form. Now many research interest moved to the next stage focusing on the control of higher-order structures using self-assembling approach based on amphiphilic molecules[9] or cross-linked metal complex[10,11] as the unit.

Dendrimers, first reported by Tomalia et al. in 1984,[12] have a unique macromolecular architecture with highly branched backbones.[13–20] Such architecture can be compared to that of a tree because the branching spreads to the outside from the focal point (core). While linear or branched polymers cannot define their structures and coordination in one limited form, macromolecular ligands based on the dendrimers can be used as a template for the precise macromolecule–metal hybridization because they have a single molecular weight and a sphere-like structure.[21–24] In general, dendrimers bearing rigid π-conjugating backbones are known to have a dense shell and a sparse core.[25,26] The nano-space around the core unit is utilized as a molecular-capsule for capturing metal ions,[27–33] clusters,[34–42] or other guest molecules.[43,44] The dendrimers can manage electron[45–47] or energy[48–58] transfer between the core and the periphery due to their unique density-gradated architecture.

One of the most typical structures of metallo-dendrimers is similar to that of metallo-proteins[59] which have a metal complex at the center of poly-peptide chains. They are mimicked by dendrimers bearing metal complexes as the core unit located at center of the molecule (Type A: Fig. 1).[60,61] Molecules belonging in this type show a large "environment" effect in general. In addition, this type of dendrimer complex has one

Published on the web April 7, 2006; DOI: 10.1246/bcsj.79.511

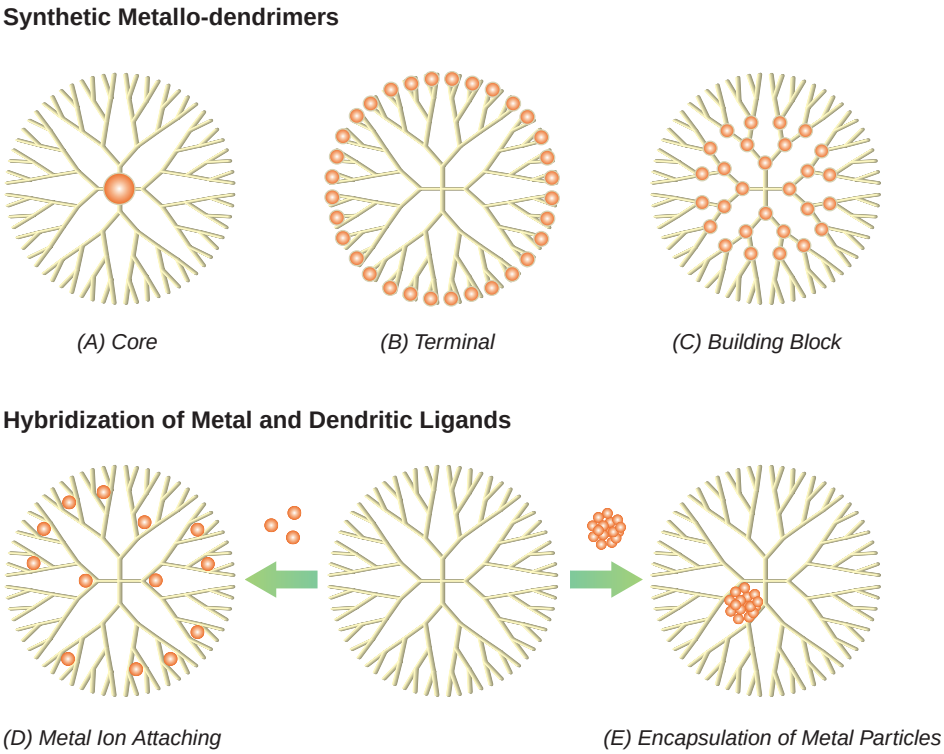

Fig. 1. Preparation strategies to metallo-dendrimer nano-composites. Synthetic routes enable formation of the stable and mono-structured metallo-dendrimers, although they are limited in selections of the metallic element and their architecture. Hybridization routes provide methodology of instant preparation for various metallic cation and nano-particles. They include formation of some structural isomers in general depending on their hybridization conditions.

limited hybrid structure and conformation, thus the nano-environment around the metal center can be regarded to be unity.[62,63] The type A dendrimers with a metallo-porphyrin core in particular are utilized as a mimic of enzymatic reactions and shape selective catalysis, utilizing the unique reaction fields.[43,64–66]

On the other hand, peripheral terminals are exposed to the outside, providing the opposite character to the core. Dendrimers modified by metal complexes on the peripheral terminals (Type B: Fig. 1) are usually employed as nano-sized supports for molecular recognition[67–70] or highly reactive catalysts.[71–76] Due to the dense shell character of the rigid dendrimer, modified complexes in the type B dendrimers often show a "concentration" effect of these functional centers. This type also has one limited hybrid structure and conformation similar to that of the "type A" dendrimers.[77,78]

The dendritic backbones, which can be compared to branches in a tree, are important for characterization of the dendrimer properties such as electrochemical response[79–86] or photo-reactivity,[87–97] although the backbones do not usually play a central role as the functional center. Modification of the backbones by metal ions should result in drastic changes in the entire conformation, in the environment around the core and in the electronic properties of the dendrimers. This could be regarded as a result of the environment, conformation, and concerted effect. Such modification could be done in two ways: (Type C) preparation of metal complexes incorporated as the building units,[51,98,99] and (Type D) complexation of metal ions to dendrimer ligands.[27–33] The former way provides a completely defined structure of the organometallic hybrids, but has the limitation that available structures and applications are few. The latter way can be applied to various metallic elements not only in static complexes, but also in dynamic coordination systems such as metal cluster synthesis.[34–40] However, the hybrid structure of metals and dendrimers in substance cannot be defined to one limited form until all the coordination sites in the dendrimer were filled by metal ions (Scheme 1). Because the environment for each generation (layer) of the dendrimer is not the same, the complexes in each generation are chemically different. This means a loss of structural unity in the metal–dendrimer hybrid. In addition, even the number of loaded metal ions in dendrimer molecules should have a statistical dispersity. When metal clusters were synthesized using normal dendrimer ligands, one should find some dispersity in the cluster size.

An advantage to use the dendrimer architecture for the macromolecule–metal hybridization is that the micro domain around each metal center is tunable in topological molecular design. They contribute not only to the intramolecular-level control, but also to the extended mesophase structure as a building unit. The fact recently attracts much attention because it should become a powerful tool to build a hierarchical structure across nanometer and micrometer scales. Needless to say, the metallo-dendrimer would be positioned to a unit cell for macromolecule–metal hybrid composites. The most important feature of this procedure is almost complete independence between the designing of each phase in molecular unit (functional center), local domain (dendrimer), and extended struc-

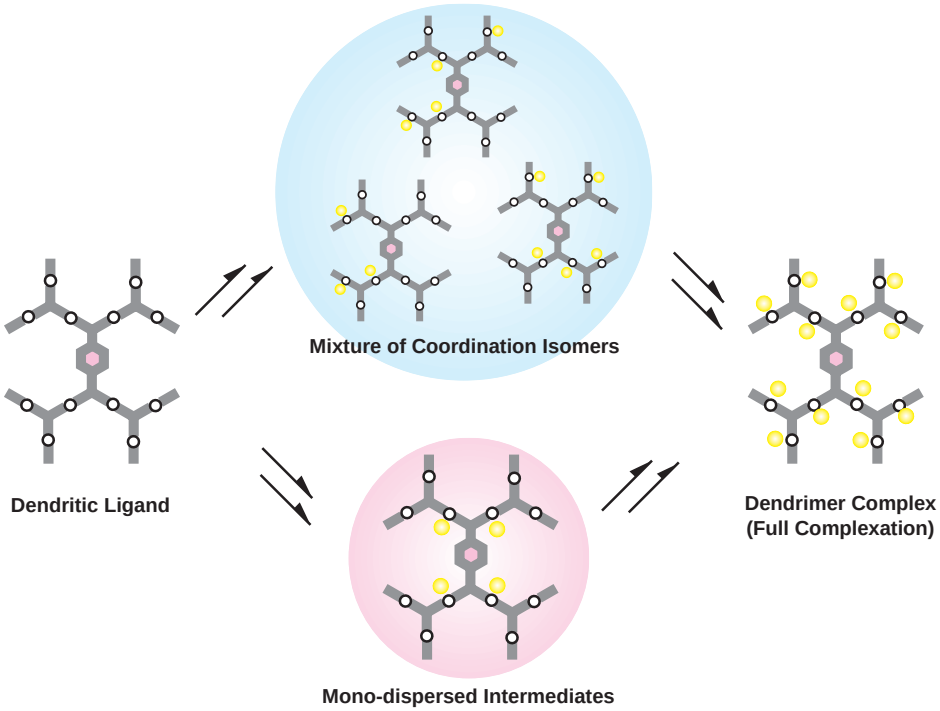

Scheme 1. Schematic representation of building strategies to a type D metal–dendrimer hybrid. A metallo-dendrimer prepared from complexation of a dendritic ligand in general involves many half-coordinating isomers until the full complexation (upside path). If the coordination are controlled in order to bind the metal ion to core-side ligands prior to the terminals, the isomer would not appear (downside path).

ture (molecular assembly). To establish the entire process, a universal way to decorate various metallic elements finely to the dendrimer is a key process. This account mainly focuses on this point on the basis of a unique multi-coordinating dendrimer in which metal complexes finely recognize the site to coordinate.

2. Basic Theory of Multi-Coordination Systems

If there were macromolecular ligands that can assemble metal ions with a finely controlled stepwise process, the resulting metal assembly should have much smaller dispersity than one that results from random coordination system. As a typical example, we assume a model system in which coordination sites are arranged to form a dendritic chain. The number of the coordination sites is doubled by stepping the generations (max 4th generation) in the dendrimer model. The coordination sites in the same generation are placed in the same coordination environment due to their topological character, while the environment in different generations is not identical. Here, we define four individual coordination reactions and their constants (K_a–K_d), which correspond to each generation (layer) in the dendrimer model.

$$\text{Core:}\quad \mathrm{A} + \mathrm{M} \rightleftharpoons \mathrm{AM}\ (K_a = [\mathrm{AM}]/[\mathrm{A}][\mathrm{M}],\ [\mathrm{A}]_0 = [\text{dendrimer}]). \tag{1a}$$

$$\mathrm{B} + \mathrm{M} \rightleftharpoons \mathrm{BM}\ (K_b = [\mathrm{BM}]/[\mathrm{B}][\mathrm{M}],\ [\mathrm{B}]_0 = 2[\text{dendrimer}]). \tag{1b}$$

$$\mathrm{C} + \mathrm{M} \rightleftharpoons \mathrm{CM}\ (K_c = [\mathrm{CM}]/[\mathrm{C}][\mathrm{M}],\ [\mathrm{C}]_0 = 4[\text{dendrimer}]). \tag{1c}$$

$$\text{Terminal:}\quad \mathrm{D} + \mathrm{M} \rightleftharpoons \mathrm{DM}\ (K_d = [\mathrm{DM}]/[\mathrm{D}][\mathrm{M}],\ [\mathrm{D}]_0 = 8[\text{dendrimer}]). \tag{1d}$$

As shown in a previous paper,[100] the concentration profiles of all free ligands ([A]–[D]) and metal ion ([M]) after reaching equilibrium can be calculated for given initial concentrations of the dendrimer ($[\text{dendrimer}]_0$) and metal ions ($[\mathrm{M}]_0$). The profiles of the coordinated ligands against the added metal ion are shown in Fig. 2. If all the coordination constants were identical (Case 1: $K_a = K_b = K_c = K_d = 10^6\,\mathrm{mol^{-1}\,L}$), the metal ions would be equally distributed to all ligands (A, B, C, and D) at any molar amount of addition. In this case, the number of metals in one dendrimer molecule would have a statistical distribution until the coordination sites are completely filled by added metal ions. For example, the metal ions are equally distributed to each layer depending on the number of coordination sites in each layer on the midway (5 molar amounts) to the full complexation (Table 1). In contrast, the coordination profiles were changed by down slope of the coordination constants (Case 2: $K_a = 10K_b = 100K_c = 1000K_d = 10^7\,\mathrm{mol^{-1}\,L}$). At the initial point of the addition, the distribution priority to the core-side layer is higher than that to the outer layer, and then the prior coordination site is gradually moved to the outer layer. If 5 molar amounts of metal ion were added to the dendrimer, 89% (4.46/5) of added metal ion is distributed to the inner three layers. The behavior became striking when a larger gradation of the constants are assumed (Case 3: $K_a = 10^2K_b = 10^4K_c = 10^6K_d = 10^{10}\,\mathrm{mol^{-1}\,L}$). In this case, the added metal ions clearly distinguish the sites to which they should coordinate. At the initial stage ($0 < [\mathrm{M}]_0/$

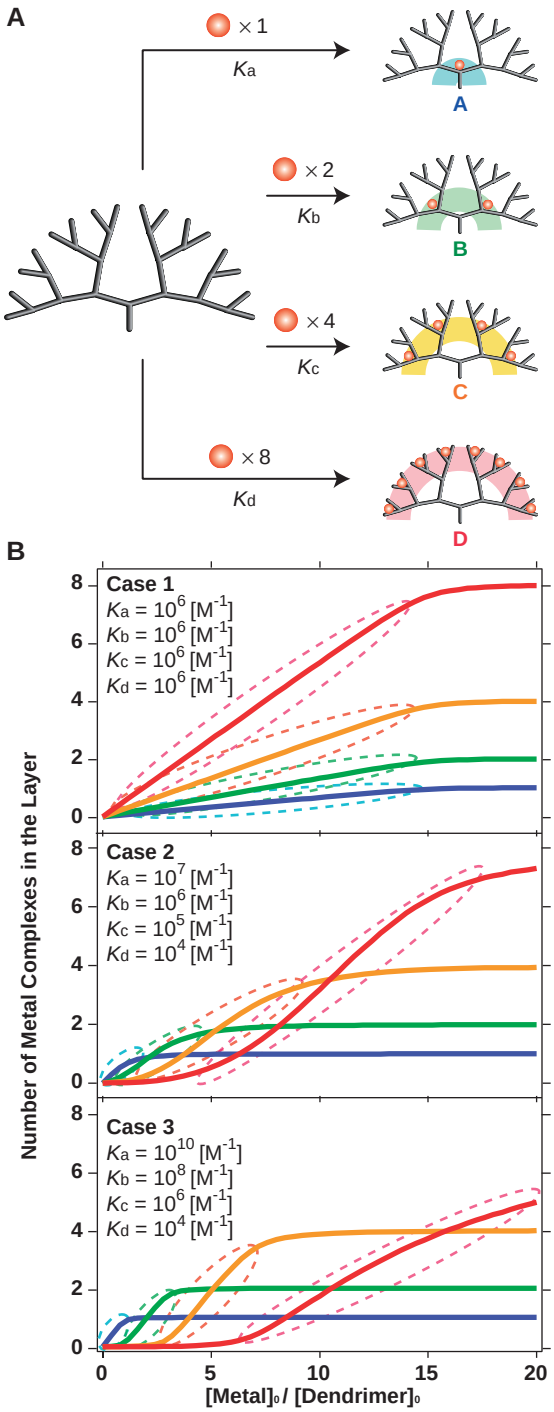

Fig. 2. (A) A model of multi-coordination equilibrium system based on a four layered dendrimer. Definition of four independent equilibria enables calculations of the entire complexation status for given coordination constants. (B) Calculated profiles of the number of metal complexation in each layer versus the added equivalent ratio of the metal ion for three different situation. Assumed concentration of the dendrimer is 2×10^5 mol^{-1} L and the number of coordination sites in each layer is 1, 2, 4, and 8.

$[\text{dendrimer}]_0 < 1$), most of the metal ions were assembled to the core-side layer (A). After the filling of layer A, the coordination site moved to the next layer (B) until that layer was filled ($1 < [\text{M}]_0/[\text{dendrimer}]_0 < 3$). Again it moved to layer C ($3 < [\text{M}]_0/[\text{dendrimer}]_0 < 7$) and finally to D ($7 < [\text{M}]_0/[\text{dendrimer}]_0 < 15$). The coordination process was completely stepwise; therefore, most metal ions (99%) would be trapped within the inner three layers if 5 molar amounts of the free metal ions were added to the dendrimer (Table 1). The dendrimer model assumed in case 3 can distribute metal ions to core-side layers with higher priority. This should result in the mono-dispersity of the number of metal ions distributed to each dendrimer molecule in principle, because the statistical factor becomes negligible at each section of the molar ratio between the dendrimer and the metal ion.

Table 1. Number of Metals Distributed to Each Layer of the Dendrimers Assumed in Fig. 2 upon the Quantitative Addition of 5 Molar Amounts

Layer	Ligands[a)]	1	2	3
A	1 (1)	1.00	0.99	0.33
B	2 (2)	1.98	1.76	0.66
C	4 (2)	1.90	1.68	1.33
D	8 (0)	0.07	0.54	2.66

a) Values in the parentheses are the number of metals distributed to each layer if the ideal stepwise coordination was occurred from the core side.

3. Fine-Controlled Metal Assembling in DPAs (Dendritic Phenylazomethines)

As shown in the previous section, the complexation randomness within the dendritic architecture should be removed if the constants of the metal assembling could be gradated by layers. A design strategy for such an unusual system is to utilize the unique dense shell property of rigid dendrimers.[25,26] All dendrimers reported as ligands for multi-metal ion assemblies have flexible backbones composed of single covalent (σ) bonds. However, they are not suitable for precise metal assembly because their conformational changes and back-folding with thermal vibrations would prevent the precise discrimination of the coordination sites.[81] We reported some dendritic ligands which have fully aromatic π-conjugating backbones.[101,102] The dendritic phenylazomethines (DPAs) shown in Fig. 3 behave as unique dendritic ligands, in which various metal ions were assembled to the imine nitrogen (C=N) from the core-side layer in an orderly fashion.

An example of the stepwise complexation about the simplest DPA (**Ph-DPA G4**) with $SnCl_2$ is explained below.[100] $SnCl_2$ acts as a Lewis acid and forms a 1:1 complex with each imine (C=N) in the **Ph-DPA G4**. This is confirmed by the model compound (**Ph-DPA G1**) bearing only one imine unit. Because the complexation accompanies a significant change in the π–π^* transition energy, it can be monitored by measurements of the UV–vis absorption spectra upon the addition of $SnCl_2$. The spectral change saturating up to the addition of 1 molar amount of $SnCl_2$ means a 1:1 complexation between the phenylazomethine unit and $SnCl_2$. It can also be determined by the Job titration method, showing the maximum absorption change at the 1:1 mixing ratio. A similar UV–vis titration was also applied to the **Ph-DPA G4** bearing 15 imines within one dendrimer (Fig. 4). This material showed a signifi-

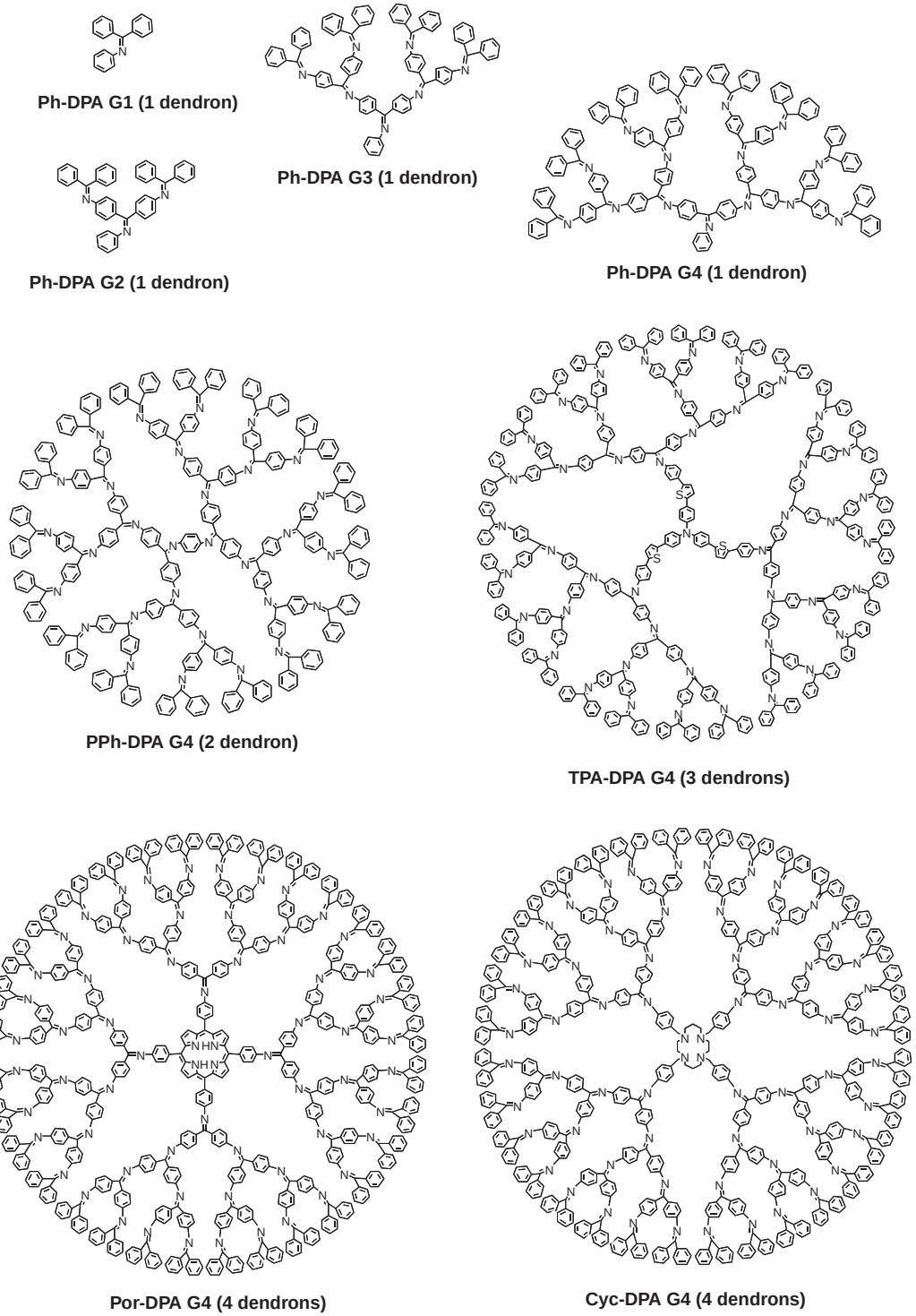

Fig. 3. Structures of DPAs having various core units.

cant change in the UV–vis absorption on the addition of $SnCl_2$. The spectrum of **Ph-DPA G4** gradually changed with an isosbestic point at 371 nm up to the addition of 1 equimolar amount versus the molar concentration of the dendrimer. The isosbestic point then shifted upon the further addition of $SnCl_2$, and appeared at 368 nm between 1 and 3 equimolar amounts. During the addition of $SnCl_2$ from 3 to 7 equimolar amounts, the isosbestic point appeared at 363 nm, and finally it moved to 360 nm with the addition of more than 7 equimolar amounts. Overall, the isosbestic point shifted about 11 nm from 371 to 360 nm.

These results observed during the titration strongly suggest a stepwise process of multiple coordination reactions. If the entire coordination proceeded simultaneously, only one isosbestic point should be observed during the titration because the spectral change would appear as an average of all the reac-

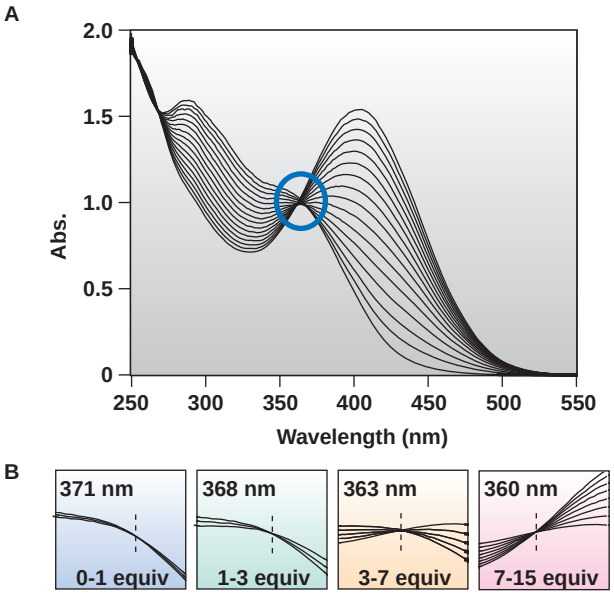

Fig. 4. (A) The UV–vis spectral change upon the addition of $SnCl_2$ to **Ph-DPA G4**. (B) Enlargements of the isosbestic points appeared successively with displayed equimolar amounts of $SnCl_2$.

tions. In this system, four different isosbestic points appeared in turns starting from each section at 0, 1, 3, and 7 equimolar amount additions; and continued until the next section (finished at 15 molar amounts). In addition, the number of equimolar amounts between each section (1, 2, 4, and 8) completely agreed with the number of imines in each layer of the **Ph-DPA G4**. The coordination profiles about each layer should be those shown in Fig. 2.

A similar stepwise radial complexation was observed for the DPA derivatives (Fig. 3). When $SnCl_2$ was added to the solution of these dendrimers, four isosbestic points were successively observed in the spectra. In **PPh-DPA G4** bearing two dendrons (Fig. 3), each shift occurred with the repeated additions of 2, 4, 8, and 16 equimolar amounts of $SnCl_2$.[103,104] On the other hand, **TPA-DPA G4** bearing three dendrons (Fig. 3) showed distinct shifts with the repeated additions of 3, 6, 12, and 24 equimolar amounts,[105] while **Por-DPA G4**[106] and **Cyc-DPA G4**[107] (Fig. 3) bearing four dendrons showed the distinct shifts with 4, 8, 16, and 32 equimolar amounts of addition. In each dendrimer, the equimolar amounts of $SnCl_2$ added to the solution needed to shift the isosbestic point also agreed with the number of imines in the 1st to 4th shells. These results support the conclusion that the complexation in the DPA derivatives proceeds from the core-side imines to the terminal ones, as shown in Scheme 2. The stepwise reaction is also evidenced by several methods (transmission electron microscope, electrochemical measurement of coordinating iron complexes, and product analysis on metal assisting reduction of imines).[104,108]

From a kinetic standpoint, complexation of the terminal imines in the dendrimer is expected to occur first. However, the results suggest that, on the time scale of our observations, the process is thermodynamically controlled. As a possible explanation of the stepwise complexation, we propose two mech-

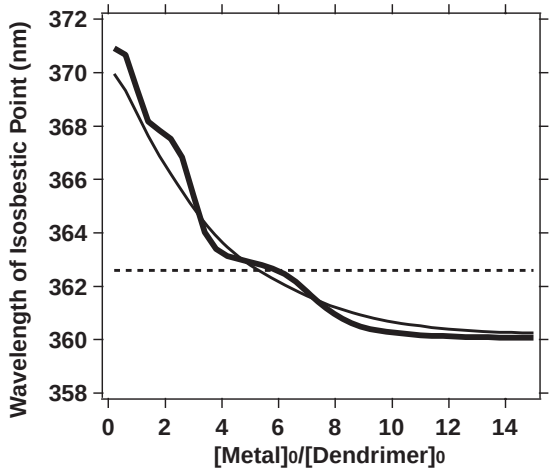

Fig. 5. Calculated changes in isosbestic point for three different conditions in the coordination constants assuming the same system treated in Fig. 2. Bold line corresponds to strongly stepwise system in which the coordination constants in each layer is gradated by a 100 times difference ($K_a = 10^2K_b = 10^4K_c = 10^6K_d = 10^{10}$ mol^{-1} L). Normal line corresponds to stepwise system in which the coordination constants in each layer is gradated by 10 times difference ($K_a = 10K_b = 100K_c = 1000K_d = 10^8$ mol^{-1} L). Dotted line corresponds to the equally coordinating system in which all the coordination sites have the same constants ($K_a = K_b = K_c = K_d = 10^6$ mol^{-1} L).

anisms. One is a steric factor based on the dense shell architecture of the dendrimer. It is possible that the coordination to the outer layers is prevented due to the clouded environment. However, this mechanism is insufficient to explain all results, because the steric factor generally decreases the coordination constant. Another explanation is that the basicity gradient of the imines from layer to layer is caused by an electronic effect. This is demonstrated by the effect of substitutions on the core versus the coordination behavior. For example, **F_4PPh-DPA G3** in which the *p*-phenylene core is substituted by four electron-withdrawing fluoro groups showed different changes in the isosbestic point from the analogue without fluoro groups (**PPh-DPA G3**).[102–104] Although the usual behavior (shifts of the isosbestic point upon the repeated addition of 2, 4, and 8 molar amounts of $SnCl_2$) was observed for **PPh-DPA G3**, the isosbestic point during the titration of **F_4PPh-DPA G3** was shifted upon the addition of 4, 8, and 2 molar amounts of $SnCl_2$. This indicates that $SnCl_2$ initially coordinates to four imines in the second shell (intermediate), then coordinates to the eight imines in the third shell (terminal), and finally coordinates to two imines in the first shell (core) as shown in Scheme 3. In the DPA derivatives, it is likely that a native basicity gradient is formed due to the electron-donating effect from the outer imine units, and that this gradient is variable by attaching electron-withdrawing groups.

4. Simulations of the Isosbestic Point

For the quantitative evaluation of the complexation, we have to know how much of a difference between neighboring coordination constants (K_C) is required for the stepwise shift in the isosbestic point. To estimate the profile of the isosbestic

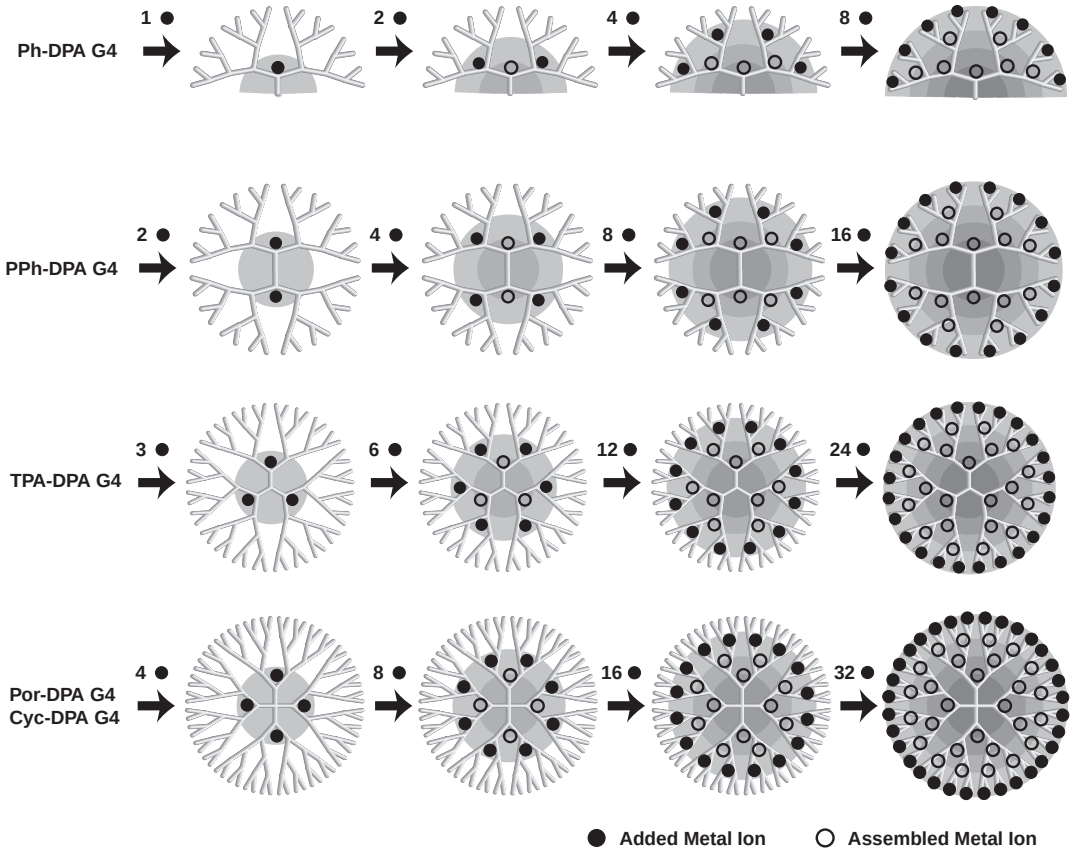

Scheme 2. Schematic representations of stepwise complexation in DPAs.

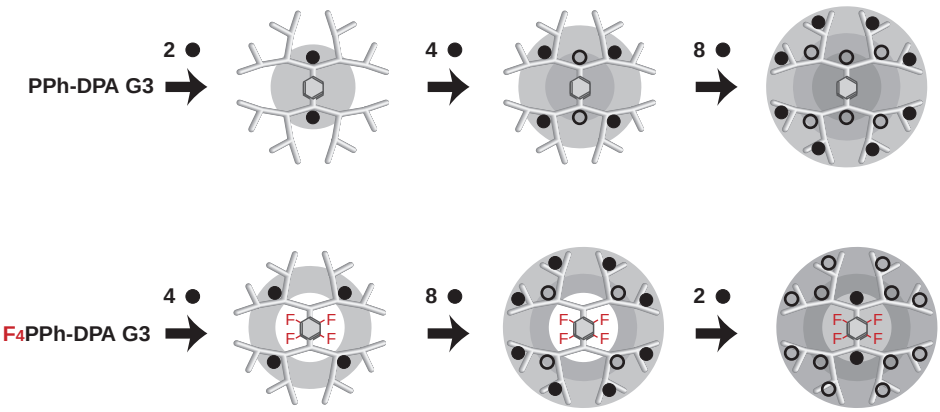

Scheme 3. Schematic representations of stepwise complexation in DPA G3s bearing *p*-phenylene or tetrafluoro-*p*-phenylene core.

point, we use the theoretical concentration profile again. A UV–vis absorption coefficient (ε) is generally written as a function of the wavenumber with a Gaussian expression. The function of the wavelength (λ) is given by:

$$\varepsilon(\lambda) = \varepsilon^{\circ} \exp\left\{\frac{-\delta(1/\lambda^{\circ} - 1/\lambda)^2}{kT}\right\}, \quad (2)$$

where λ° is the wavelength at the absorption maximum, ε° is the absorption coefficient at $\lambda = \lambda^{\circ}$, and δ is the thermal vibration parameter of the chromophore. The observed absorbance (A) should be the sum of these functions, therefore, we assigned one function to each phenylazomethine unit in every layer (either complex and free base). For ease of calculation, the parameters of these absorptions (ε° and δ) were set to the same value for each chromophore. The absorbance change (ΔA) involved in the small addition of the metal ion ($\Delta[\mathrm{M}]_0$) is then given by:

$$\Delta A(\lambda) = \varepsilon^{\circ} \sum_{\mathrm{N}} \left[\Delta[\mathrm{N}] \exp\left\{\frac{-\delta(1/\lambda_{\mathrm{N}}^{\circ} - 1/\lambda)^2}{kT}\right\} + \Delta[\mathrm{NM}] \exp\left\{\frac{-\delta(1/\lambda_{\mathrm{NM}}^{\circ} - 1/\lambda)^2}{kT}\right\}\right], \quad (3)$$

as the sum of each component (N = A, B, C, and D, meaning the coordination sites in each layer) using the calculated value of the concentration profiles (Fig. 2). Based on the definition,

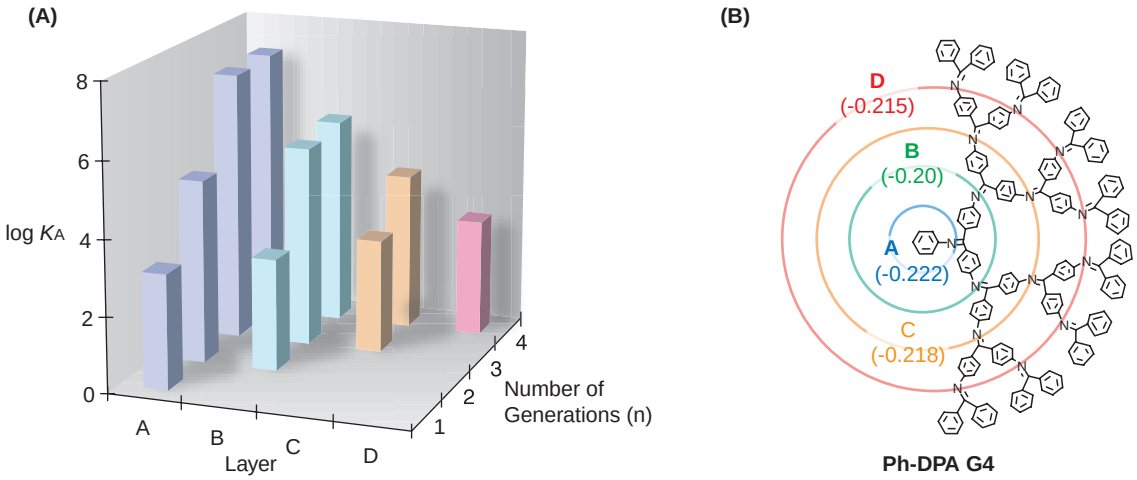

Fig. 6. (A) Association constants of proton (TFA) to imine sites in each layer of the phenylazomethine dendrimers (**Ph-DPA G*n***: $n = 1$, 2, 3, and 4) obtained by fitting of simulation results into the experiment (titration). All experimental value were obtained in chloroform/acetonitrile (v/v = 1/1) solution. (B) These values in parentheses are calculated Mulliken's charge population on imine nitrogen in each layer of **Ph-DPA G4**. The electron negativity of imines closer to the core is higher than that of the outer imines. The DFT calculation using STO3G was done with Gaussian 03 software (rev. C.02).[124]

the isosbestic points were calculated as a λ solution of the equation $[\Delta A(\lambda) = 0]$. The simulated profiles of the isosbestic point for the assumed λ° values are shown in Fig. 5. When the coordination constants (K_C) for each layer are the same value (Case 1), the isosbestic point was fixed for every molar amount of the added metal ion. In contrast, the isosbestic point shows a stepwise change during the addition if the K_C values were set to Case 3, where each K_C for the layers were gradated by a 100 times difference. If the difference in K_C is smaller (Case 2), the change in the isosbestic point becomes continuous.

The results shown in the simulation demonstrate that the coordination constants (K_C) in the DPA experiments should have a considerable difference when the constants of neighboring layers are separated by more than two orders of magnitude.

5. Basicity of the Imine Units in DPAs

A driving force that discriminates between the complexations to each layer is considered to include a combination of the steric and basicity factors. To reveal the basicity gradient within the DPA structure, we evaluated the protonation of **Ph-DPA G*n*** ($n = 1$, 2, 3, and 4) by spectroscopic titration using trifluoroacetic acid (TFA).[100] The data were also recorded as spectral changes with isosbestic points using the same setup for the titration with $SnCl_2$. The association constants (K_A) of protons to each imine were characterized by simulation of the spectral changes. At first, the experimental change in the isosbestic point was fitted by the simulated one, which can be calculated by the method described in the previous section. The unknown parameters such as λ° or δ were obtained from the differential spectra upon the addition of a small portion of TFA. Because the protonation also proceeds in a stepwise reaction, we could separately determine the parameters for each layer of the dendrimers by monitoring each section during the titration. The method using the isosbestic point is efficient for determining the difference in the constants between each layer, but cannot fully characterize the absolute values. Thus, we have to include the other method using the absorbance change until saturation of the protonation upon the addition of an excess amount of TFA. The hybrid method was applied to a series of mono-dendronized **Ph-DPA G*n*** ($n = 1$, 2, 3, and 4) in order to determine all the association constants of each dendrimer.

As shown in Fig. 6A, obtained values indicate that there is a gradient in the basicity of the imine sites by the layers. The association constant for the core-side one is obviously enhanced; the basicity proved to be extraordinarily high ($\log_{10} K_A \approx 7$). In contrast, these values of the terminal imines are roughly of the same order ($\log_{10} K_A \approx 3$) as those of **Ph-DPA G1** for all the Ph-DPAs. The unique property of the basicity can be explained by the gradient of the electron density. Due to the topology of the dendrimers, each nitrogen terminal of the imine unit (C=N) is arranged in the core direction. Therefore, the electron-donating effect due to the outer imine units is amplified by increasing the generation number of the dendrimer, which results in a higher electron density in the core-side shell. It is also shown as Mulliken (charge) population estimated by a molecular orbital calculation for **Ph-DPA G4** (Fig. 6B). The averaged electron negativities on the nitrogen atoms for each layer indicate an enhancement in the electron density for the inner shells.

The coordination constant (K_C) of **Ph-DPA G1** with $SnCl_2$ was determined to be $9.5 \times 10^4\ mol^{-1}\ L$ in dichloromethane/acetonitrile. The K_C value is about 100 times greater than the association constant (K_A) with TFA (proton). On the basis of this result, the coordination constants of $SnCl_2$ with **Ph-DPA G4** for each generation are postulated to be two orders of magnitude greater than that of TFA. In addition, other metal ions, such as iron and lanthanides, are applicable to a similar assembly in the DPAs, and their coordination constants depend on the Lewis acidity of the metal ions.

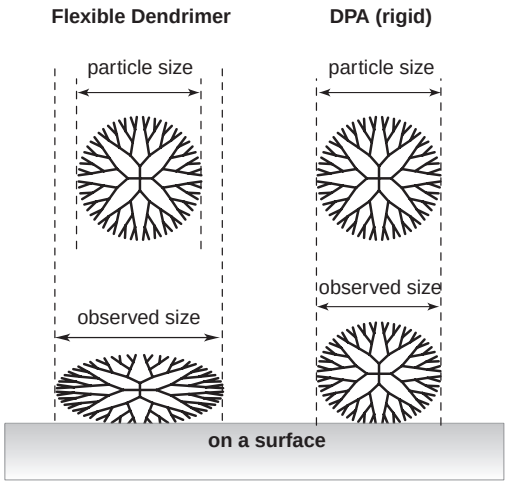

Fig. 7. Flexible dendrimers such as PAMAMs are deformed on a plate surface whereas DPAs keep their conformation due to the rigidity. This can be compared by the size observed in TEM image. PAMAMs showed much larger diameters than that predicted in solution. A diameter of the **PPh-DPA G4** on a surface is much smaller than that of PAMAMs.

6. Physical Properties of DPAs in a Solid Phase

A **PPh-DPA G4** molecule bearing two dendrons was confirmed by FE-TEM (field-emission transmission electron microscopy) as a stained image by RuO_4. The observation revealed that the dendrimer has a round shape with a 2.3 ± 0.3 nm diameter.[101,102] It is noted that such a 2.3 nm diameter is much smaller than that of a reported dendrimer such as PAMAMs with a similar number of generations.[109] In the dendrimers having a single-bonded backbone, the diameter observed by TEM is much larger than expected, because the flexible backbones of the dendrimers cause deformation of the molecule on a plate (Fig. 7). In other words, the smaller diameter of a **PPh-DPA G4** molecule shows a three-dimensionally expanded structure without any deformation. However, the TEM images do not provide information about the height. In order to reveal the height of the **PPh-DPA G4** on a plate surface, AFM (atomic force microscope) observations are performed in the non-contact mode. The **PPh-DPA G4** molecules are observed by AFM to be regularly assembled in a multi-layered packing structure on a graphite surface only by simple solvent casting. A lattice pattern is observed in the image and the cross section clearly shows alignment of the spherical molecules in a multilayer. The height of the **PPh-DPA G4** molecule is estimated from the cross section to be at least 2.0 ± 0.1 nm. Interestingly, **PPh-DPA G4** molecules are assembled without deformation of the molecule on a plate because of the conformational rigidity.

Linear poly-phenylazomethine compounds are known to have stability against heat decomposition.[110] However, they are nearly insoluble in most organic and inorganic solvents. Thus, their fundamental properties are still unknown, and they are not applied in practical use. The dendritic phenylazomethines (DPAs) are unexpectedly soluble in most organic solvents and also have a resistive property against heat decomposition.

Table 2. 10% Weight-Decreasing ($T_{d\text{-}10\%}$) and Glass-Transition Temperatures (T_g) of Phenylazomethine Dendrimers

Dendrimer	$T_{d\text{-}10\%}$/°C	T_g/°C
PPh-DPA G1	≈400	50
PPh-DPA G2	514	148
PPh-DPA G3	511	174
PPh-DPA G4	521	188
Por-DPA G1	531	—[a]
Por-DPA G2	528	—[a]
Por-DPA G3	523	195
Por-DPA G4	531	201

a) No clear phase transition was observed.

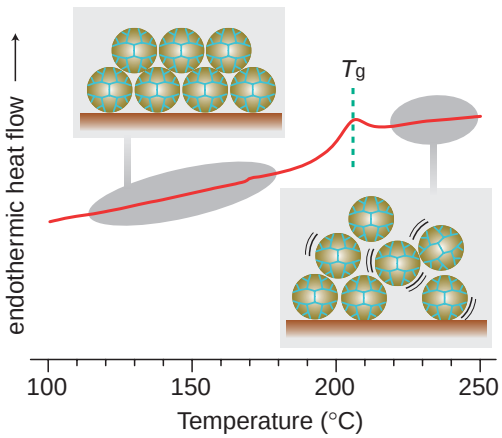

Fig. 8. A heat flow curve obtained by a differential scanning calorimetry (DSC) measurement of **Por-DPA G4** during the heating process at the scan rate of 40 °C min^{-1}. The curve clearly shows a glass transition at 201 °C. It should correspond to the transition between the packing and moving state of the dendrimer solid.

The 10 wt %-decreasing temperatures ($T_{d\text{-}10\%}$) of **PPh-DPA G*n*** ($n = 2$, 3, and 4) are higher than 500 °C (Table 2).[111] This property is based on the π-conjugating backbone of the DPAs, which is chemically stable. It is noteworthy that the temperature is higher than those of the linear poly-phenylazomethines. This result should be related to the high density of the molecular unit in the backbones of the dendrimers. This is not an exception and is also observed with **Por-DPA G*n*** ($n = 1$, 2, 3, and 4).

While $T_{d\text{-}10\%}$ does not show a clear dependence with the number of generations in the dendrimers, the glass-transition temperature (T_g) obviously increased with the number (Table 2).[111] Amorphous solids of **PPh-DPA G4** or **Por-DPA G4** have an exceptionally high T_g (201 °C) relative to that of aromatic poly-ether dendrimers.[112] This means that the packing structure of the DPAs, which was observed by AFM, is very stable due to their rigid backbones (Fig. 8). Such a good thermostability is almost equal to those of engineering plastics. Due to their high solubility, DPAs have potential applications for easy preparation of thermostable polymer films by spin casting or ink jet methods. This should be an advantage in solid-state electronic devices such as organic light-emitting diodes (OLEDs), photo diodes, and field effect transistors (FET).

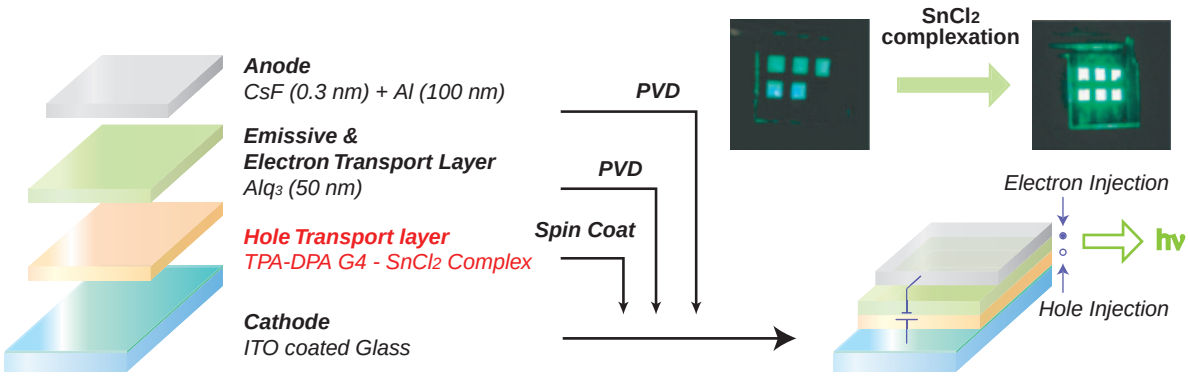

Fig. 9. An OLED cell fabricated with **TPA-DPA G4** as a hole-transport layer. The maximum luminance was obviously improved by the complexation of $SnCl_2$.

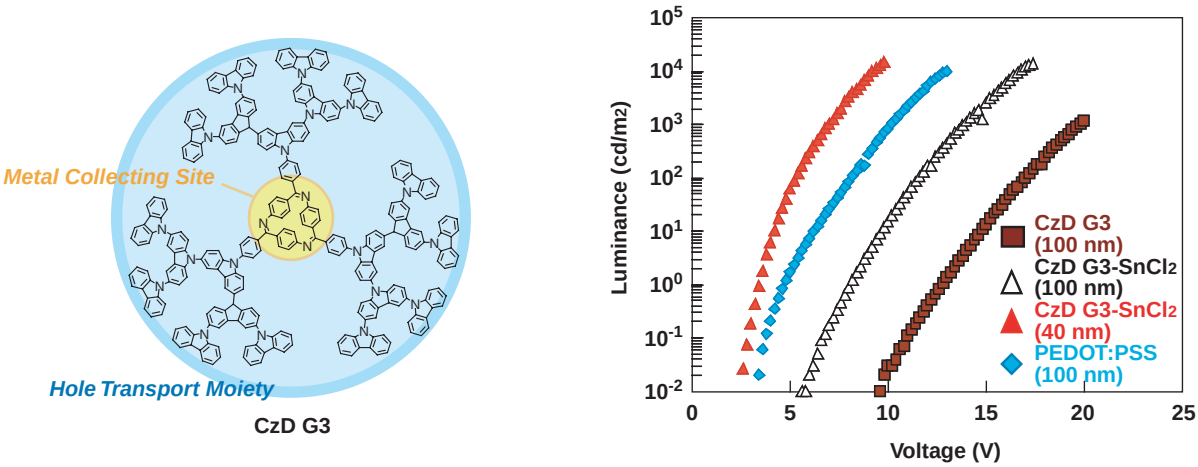

Fig. 10. (Left) A carbazole dendrimer with metal collecting site. (Right) The OLED property using **CzD G3** as a hole-transport layer.

7. Applications

7.1 Organic Light-Emitting Diodes. Triarylamines play an important role as a hole-transport material in electronic devices such as organic light-emitting diodes (OLEDs) and photo cells.[113,114] However, their monomeric molecules do not exhibit a high hole-transport efficiency because of their crystallinity, low mobile ability, or low thermal stability. Convenient solution processing has also been desired for the preparation of these devices with a large area. Dendritic macromolecules having a sphere-like and rigid structure make them easy to prepare as a homogeneous film by solvent casting. To make the dendritic molecule act as an efficient hole-transport compound, a novel charge-transport system needs to be constructed through the dendron shell between the hole-transport core.

TPA-DPA G*n* ($n = 1$, 2, 3, and 4) are applicable as a hole-transport material in an electro-luminescence (EL) device, using the metal-assembling properties in which the metal acts as a mediator of the hole transfer.[105]

The OLEDs were fabricated; we employed the **TPA-DPA G*n*** ($n = 1$, 2, 3, and 4) or their complexes with $SnCl_2$ as the hole-transport materials and tris(8-hydroxyquinoline)aluminum (Alq) as the luminance layer (Fig. 9). The fine-controlled metal complex with one $SnCl_2$ in the TPA-DPAs acts as a hole-transport material, whereas the TPA-DPAs without the metal complex do not show this property. The OLED cell composed of the metal complex with **TPA-DPA G4** shows ca. 1200 cd m^{-2} of luminescence at 10 V. As a result, the EL performances of the devices using the TPA-DPA metal complexes are drastically increased (20 times) by the metal complexation.

The synergetic effect obtained by adding the metal ion is not a special case of **TPA-DPA G4** with $SnCl_2$. In order to improve the EL performance, carbazole dendrimers (CzDs) with metal collecting sites were also employed as novel hole-transport materials.[115] The carbazole dendrons in the CzDs act as a more efficient hole-transport moiety than those of the phenylazomethine units. For the two-layer OLEDs, films of the dendrimer complexes (CzD) with $Eu(OTf)_3$ (europium tris(trifluoromethanesulfonate)) were then employed as the hole-transport layer. The low driving voltage and enhanced efficiency were followed by the simple assembling of the metal ions. For the G3 dendrimer of the CzDs, the turn-on voltage was reduced from 4.3 to 3.7 V and the maximum luminescence was enhanced from 786.4 to 932 cd m^{-2} by only complexing with $Eu(OTf)_3$. Also, the current performance of the **CzD G3** complex was over three times greater (181.4 mA cm^{-2}) for the same forward driving voltage (10 V) compared to the uncomplexed device (53.6 mA cm^{-2}) (Fig. 10). By inserting a thin CsF layer between the anode and electron-transport layer (Alq), a significant improvement in the cell performance was

obtained based on the enhancements of the electron injection from the Al electrode. For the G3 dendrimer, the maximum luminescence was enhanced from 3717 to 6718 cd m^{-2} by applying a lower voltage and only by complexation with $Eu(OTf)_3$ under non-optimized conditions. These results indicate that the dendrimer complexes act as an excellent hole-transport material for practical use.

7.2 Multi-Electron Transfer Catalyst. The conversions of small molecules such as O_2, N_2, or CO_2, are important reactions because they are fundamental resources for the productions of various organic compounds.[116] In addition, they also take very important roles in the energy-circulation system of nature. These conversions (reduction and oxidation) generally involve very large activation energy values because of the multi-electron transfer (m-ET) processes. Natural catalysts, which exist as enzymes at photosynthetic or breath reaction centers, can accelerate these m-ET reactions by a precisely assembled poly-metallic structure as a multi-redox system. Because DPAs can define their metal-assembling structure around the core (catalytic center), they are expected to act as a mono-structured m-ET catalysts assembling multiple metal complexes.

Our previous study revealed that lanthanide metal ions ($La^{3+} = Y^{3+}$, Tb^{3+}, Er^{3+}, and Nd^{3+}) assembling DPAs with a cobalt porphyrin core act as an efficient catalyst for the CO_2 electrochemical reduction with a very low overpotential.[106] Cobalt tetraphenylporphyrin (CoTPP), which is a model of the core unit, is known to catalyze the reduction.[117,118] However, the required electrode potential for the electrochemical reduction is in the highly negative region because the reaction needs to produce unstable radical species of CO_2. Actually, a cathodic current response by the CO_2 reduction was observed at the potential of the Co(0) formation (−1.8 V vs NHE) in the cyclic voltammogram of CoTPP with dissolved CO_2 (Fig. 11). The theoretical redox potential of the CO_2 multi-electron reduction is in a much more positive region than that observed. The activation energy via the CO_2 anion radical results in a very large overpotential for the electrochemical reduction. In contrast, the metal-assembling DPA with a cobalt porphyrin core showed a catalytic response toward the CO_2 reduction at the potential of the Co(I) formation (−0.7 V vs NHE). The observed reduction potential is 1.3 V higher than the theoretical standard potential via the CO_2 radical anion (−1.97 V vs NHE), so that it cannot be explained by single-electron transfer processes.

The result is easier to understand as an m-ET reaction. Phenylazomethine complexes with Tb^{3+} can act as an electron mediator to the cobalt porphyrin core. In addition, the microenvironment around the porphyrin core remains acidic by coordinating Lewis acids. It should facilitate the m-ET reduction, which does not produce the intermediate radical species (Fig. 11).[119]

The electron-exchange kinetics between the core and metal complexes should be very fast in order to accelerate the m-ET process. In the DPA complex, the timescale of the electron transfer might be much faster than nanoseconds. This can be confirmed by a fluorescence quenching experiment of the zinc porphyrin core in **Por-DPA G*n*** ($n = 1$, 2, 3, and 4).[120] Even upon the equimolar addition of $SnCl_2$ or $FeCl_3$, the fluorescence of the zinc porphyrin core is effectively quenched (Fig. 12), demonstrating that the electron transfer takes place within a much shorter timescale than the lifetime of the zinc porphyrin singlet-excited state (≈2 ns). Four-electron reduc-

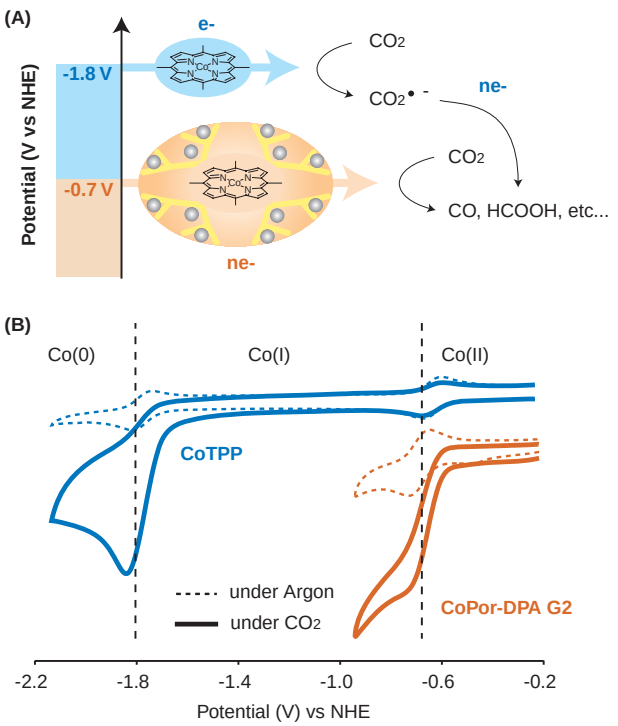

Fig. 11. (A) Catalytic CO_2 reduction by $Tb(OTf)_3$ assembling **CoPor-DPA G2** with much lower applied overpotential than CoTPP. (B) Cyclic voltammograms of CoTPP and **CoPor-DPA G2** in the presence or absence of CO_2. The cathodic current increase with CO_2 corresponds to the catalytic reduction of CO_2 mediated by the redox couple of cobalt porphyrins.

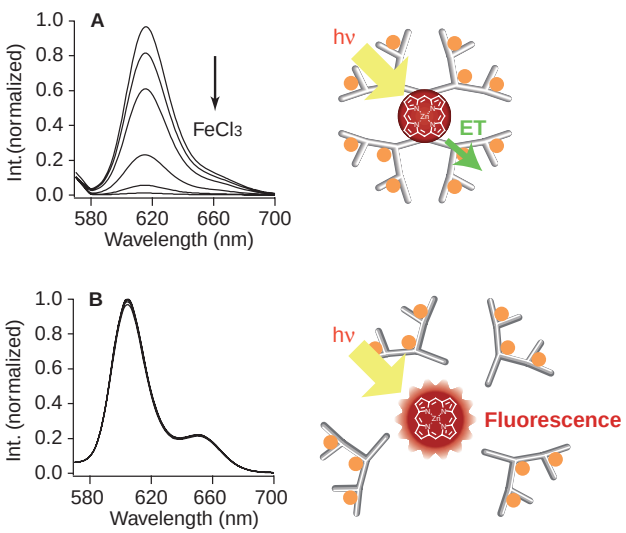

Fig. 12. Fluorescence spectra upon the addition of $FeCl_3$ to (A) **ZnPor-DPA G2** or (B) ZnTPP–**Ph-DPA G2** mixture (1/4). An effective quenching was observed only in the case of **ZnPor-DPA G2**, which indicate an ultra-fast intramolecular electron transfer within the metal-assembling structure.

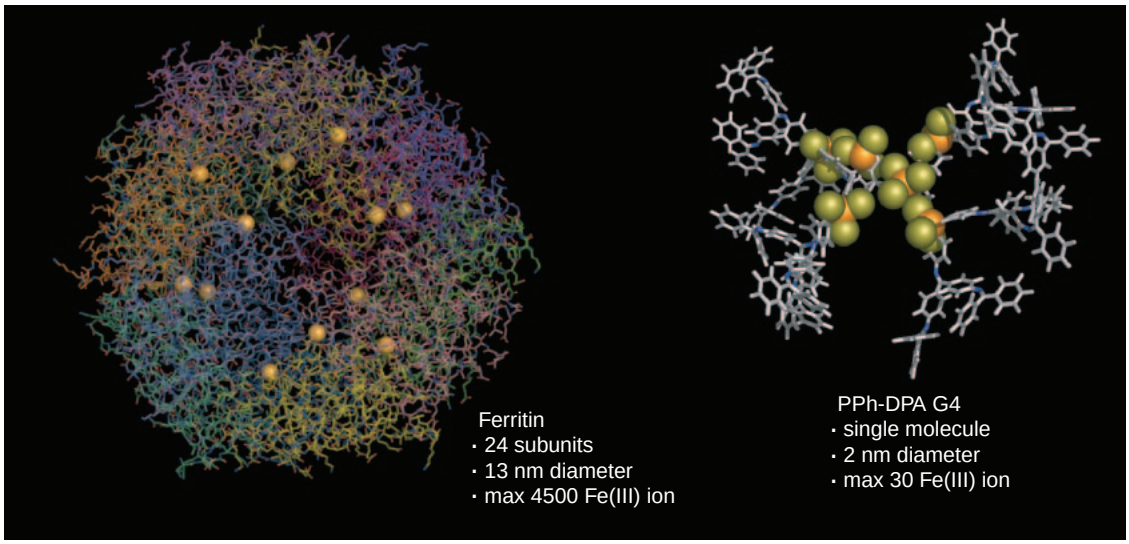

Fig. 13. **PPh-DPA G4** and Ferritin as iron storage molecules. A comparison of their structures and properties.

tion of O_2 is also promoted by the multi-nuclear cobalt porphyrin complex, in which an intramolecular electron transfer proceeds within pico-seconds.[121] The ET kinetics of the metal-assembling dendrimer system is nearly equal and could be related to the m-ET catalytic reduction.

7.3 Reversible Encapsulation and Release of Iron in DPAs. Iron is the most abundant metallic element and their complexes (heme iron or non-heme iron–sulfur cluster) in metalloproteins are indispensable for biological functions such as oxygen transport, catalysis, and redox mediation in enzymes.[59] The element is managed by[122,123] as an iron storage protein. The reversible encapsulation and release of irons in Ferritin are controlled by the oxidation states of the iron ion. We successfully demonstrated that the ferritin-like reversible encapsulation in the DPA shell is switched by the redox states of the iron ion (Fe^{2+}/Fe^{3+}).[108]

Because of the strong Lewis acidity, $FeCl_3$ effectively coordinates to the metal-assembling sites in the DPAs. The complexation of $FeCl_3$ with **Ph-DPA G1** was clearly observed using UV–vis spectroscopy as well as the complexation of $SnCl_2$. Their coordination also takes place as a 1:1 equilibrium reaction, although the coordination constant (K_C) is about $10^8\,mol^{-1}\,L$, which is 100 times greater than that of $SnCl_2$. The value was also estimated by the UV–vis titration and by the Job plot method.

PPh-DPA G4, which can take 30 equimolars of $SnCl_2$ also assembles 30 $FeCl_3$ molecules in the dendrimer shell (Fig. 13). The complexation accompanies UV–vis spectral changes through the complexation, thus the coordination process can also be analyzed by a method similar to that for $SnCl_2$. Due to the intrinsic absorption of $FeCl_3$ around 350 nm, no crossing point was observed in the raw spectral change upon the addition of $FeCl_3$. For a precise analysis of these spectra, virtual absorption spectra, in which the added $FeCl_3$ absorption was subtracted from the raw data, were examined. The subtracted spectra have a virtual isosbestic point, which displayed four wavelength in turn during the addition similar to $SnCl_2$. The numbers of the equivalents ratio required to shift the isosbestic point were also matched with the number of imine sites in each layer. Therefore, this is evidence for a stepwise reaction similar to that observed in the $SnCl_2$ coordination.

A redox driven reversible encapsulation/release switching was examined by spectroelectrochemical measurements. A quasi-reversible redox wave of (Fe^{II}/Fe^{III}) was observed at $-0.2\,V$ vs Ag/Ag^+. When the applied electrode potential was set to $-0.5\,V$ where the Fe^{III} was reduced to Fe^{II}, the absorption band at 410 nm decreased with an increase around 300 nm (Fig. 14A). The spectral change was identical with the opposite change observed during the complexation of $FeCl_3$ to **PPh-DPA G4**. The low coordination constant of $FeCl_2$ to the imine unit (ca. $0.8\,mol^{-1}\,L$ to **Ph-DPA G1**) adequately explains the decomplexation of iron from **PPh-DPA G4** through the electrochemical reduction of Fe^{III} to Fe^{II}. The conversion between each state is completely reversible (Fig. 14B). This means that the encapsulation and release of iron can be controlled by the electrochemical potential switching (Fig. 14C). The determination of the reversible assembly of multiple irons into one dendrimer is related to the function of the iron storage protein (Ferritin). This result shows one of the steps to create a novel drug delivery system using highly organized materials.

8. Concluding Remarks

The discovery of some unique complexation behavior in π-conjugating dendritic ligands provided a new methodology to construct well-defended nanostructure in one macromolecule–metal hybrid. The stoichiometric analysis using UV–vis absorption measurements enabled the quantitative evaluation of the coordination behavior. This molecule in principle enables the easy preparation of a mono-dispersed metal assembly in a macromolecule. Furthermore, the second structure of the dendrimer (molecular packing) in the amorphous solid is also stable and well-organized. We have extended these molecules and targeted the research at various applications that could not be obtained using conventional macromolecular ligands. An excellent property of these dendrimers as a hole-transport layer in an OLED cell suggests the potential use for decreasing the energy losses based on the uncertainness in a microscopic hybrid structure and the molecular ordering in the solid phase.

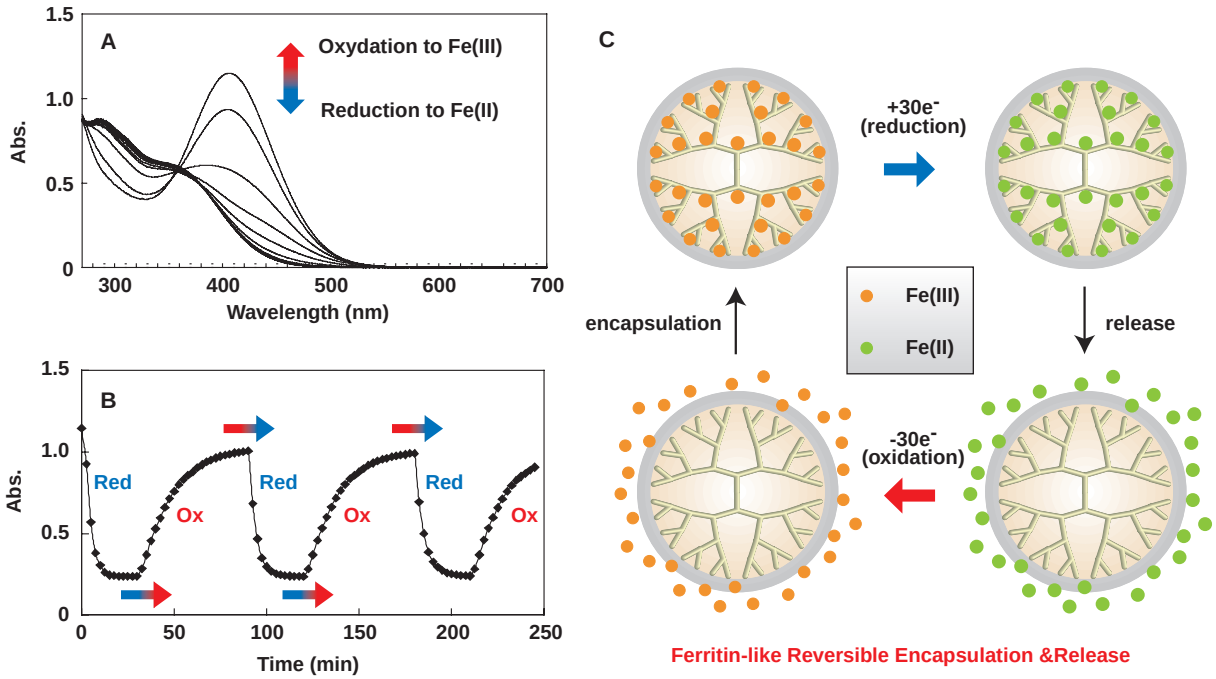

Fig. 14. Reversible assembly and release of iron chloride in **PPh-DPA G4** switched by valence state of the iron ion (Fe^{II}/Fe^{III}), (A) is the UV–vis spectral change during the electrochemical oxidation and reduction. (B) is a time-profile of the absorption change at 400 nm. (C) illustrates schematic representation of the reversible encapsulation/release cycle.

It is noteworthy that the performance of an LED cell could be drastically improved only by the addition of a few equivalents of $SnCl_2$. This fact is demonstrated by the effective doping of the hole-transporting material without any aggregation and phase separation. The synergetic enhancement of chemical functions by the metal assembling is also available in a homogeneous solution. Metal-assembling DPAs having a cobalt porphyrin core could catalyze CO_2 reduction with a 1.1 V lower overpotential than that needed for the catalysis by a model of the core (CoTPP). The CO_2 reduction facilitated by the metal assembly is explained by acceleration of the multi-electron transfer process by concentrating metal ions around the porphyrin core. Very fast electron transfer (ET) on a pico-second timescale is expected for the intramolecular ET in the dendrimer architecture. A similar mechanism is also known as inter-protein ET mediated by metal complexes held by a protein matrix. A reversible encapsulation/release of multiple iron complexes is also demonstrated as a mimic of the iron storage protein (Ferritin). Switching between the two states can be completely controlled by the redox states of the iron (Fe^{II}/Fe^{III}).

The number of metal ions in one dendrimer is mono-dispersed in principle, so that it will be applied to not only storage or a transporter, but also to metal cluster synthesis as a molecular flask, in which the number of metals is finely controlled. These materials still have great possibilities because the combination patterns of metal ions and dendrimer frameworks are many.

These studies were partially supported by CREST from the Japan Science and Technology Agency, Grants-in-Aid for Scientific Research and by the 21st COE program (Keio-LCC) from the Ministry of Education, Culture, Sports, Science and Technology.

References

1 *Macromolecule–Metal Complexes*, ed. by F. Ciardelli, E. Tsuchida, D. Wohrle, Springer, New York, **1996**.
2 R. Haag, S. Roller, *Top. Curr. Chem.* **2004**, *242*, 1.
3 N. Oyama, F. C. Anson, *J. Am. Chem. Soc.* **1979**, *101*, 3450.
4 A. Merz, A. J. Bard, *J. Am. Chem. Soc.* **1978**, *100*, 3222.
5 K. Itaya, A. J. Bard, *Anal. Chem.* **1978**, *50*, 1487.
6 S. Takeoka, H. Ohno, E. Tsuchida, *Polym. Adv. Technol.* **1993**, *4*, 53.
7 O. Kahn, Y. Pei, M. Verdaguer, J.-P. Renard, J. Sletten, *J. Am. Chem. Soc.* **1988**, *110*, 782.
8 M. Kaneko, J. Motoyoshi, A. Yamada, *Nature* **1980**, *285*, 468.
9 D. G. Kurth, N. Severin, J. P. Rabe, *Angew. Chem., Int. Ed.* **2002**, *41*, 3681.
10 S. Kitagawa, R. Kitaura, S. Noro, *Angew. Chem., Int. Ed.* **2004**, *43*, 2334.
11 B. J. Holliday, C. A. Mirkin, *Angew. Chem., Int. Ed.* **2001**, *40*, 2022.
12 D. A. Tomalia, H. Baker, J. R. Dewald, M. Hall, G. Kallos, S. Martin, J. Roeck, J. Ryder, P. Smith, *Polym. J. (Tokyo)* **1985**, *17*, 117.
13 D. A. Tomalia, A. M. Naylor, W. A. Goddard, III, *Angew. Chem., Int. Ed. Engl.* **1990**, *29*, 138.
14 M. Fischer, F. Vögtle, *Angew. Chem., Int. Ed.* **2001**, *38*, 884.
15 F. Vögtle, S. Gestermann, R. Hesse, H. Schwierz, B. Windisch, *Prog. Polym. Sci.* **2000**, *25*, 987.
16 S. Hecht, J. M. J. Fréchet, *Angew. Chem., Int. Ed.* **2001**, *40*, 74.
17 S. M. Grayson, J. M. J. Fréchet, *Chem. Rev.* **2001**, *101*, 3819.

18 A. W. Bosman, H. M. Janssen, E. W. Meijer, *Chem. Rev.* **1999**, *99*, 1665.
19 J. M. J. Fréchet, D. A. Tomalia, *Dendrimers and Other Dendritic Polymers*, John Wiley & Sons, **2002**.
20 G. R. Newkome, C. N. Moorefield, F. Vögtle, *Dendrimers and Dendrons: Concepts, Syntheses, Applications*, Wiley-VCH, Weinheim, **2001**.
21 V. Balzani, A. Juris, M. Venturi, *Chem. Rev.* **1996**, *96*, 759.
22 V. Balzani, P. Ceroni, A. Juris, M. Venturi, S. Campagna, F. Puntoriero, S. Serroni, *Coord. Chem. Rev.* **2001**, *219–221*, 545.
23 H. Frey, C. Lach, K. Lorenz, *Adv. Mater.* **1998**, *10*, 279.
24 G. R. Newkome, E. He, C. N. Moorefield, *Chem. Rev.* **1999**, *99*, 1689.
25 S. Rosenfeldt, N. Dingenouts, D. Pötschke, M. Ballauff, A. J. Berresheim, K. Müllen, P. Lindner, *Angew. Chem., Int. Ed.* **2004**, *43*, 109.
26 M. Ballauff, C. N. Likos, *Angew. Chem., Int. Ed.* **2004**, *43*, 2998.
27 M. Tominaga, J. Hosogi, K. Konishi, T. Aida, *Chem. Commun.* **2000**, 719.
28 R. J. M. Klein Gebbink, A. W. Bosman, M. C. Feiters, E. W. Meijer, R. J. M. Nolte, *Chem. Eur. J.* **1999**, *5*, 65.
29 M. F. Ottaviani, F. Montalti, N. J. Turro, D. A. Tomalia, *J. Phys. Chem. B* **1997**, *101*, 158.
30 M. F. Ottaviani, S. Bossmann, N. J. Turro, D. A. Tomalia, *J. Am. Chem. Soc.* **1994**, *116*, 661.
31 F. Vögtle, S. Gestermann, C. Kauffmann, P. Ceroni, V. Vicinelli, V. Balzani, *J. Am. Chem. Soc.* **2000**, *122*, 10398.
32 V. Vicinelli, P. Ceroni, M. Maestri, V. Balzani, M. Gorka, F. Vögtle, *J. Am. Chem. Soc.* **2002**, *124*, 6461.
33 J. D. Epperson, L.-J. Ming, G. R. Baker, G. R. Newkome, *J. Am. Chem. Soc.* **2001**, *123*, 8583.
34 R. M. Crooks, M. Zhao, L. Sun, V. Chechik, L. K. Yeung, *Acc. Chem. Res.* **2001**, *34*, 181.
35 M. Zhao, R. M. Crooks, *Adv. Mater.* **1999**, *11*, 217.
36 M. Zhao, R. M. Crooks, *Angew. Chem., Int. Ed.* **1999**, *38*, 364.
37 M. Zhao, L. Sun, R. M. Crooks, *J. Am. Chem. Soc.* **1998**, *120*, 4877.
38 V. Chechik, R. M. Crooks, *J. Am. Chem. Soc.* **2000**, *122*, 1243.
39 L. Balogh, D. A. Tomalia, *J. Am. Chem. Soc.* **1998**, *120*, 7355.
40 H. Lang, R. A. May, B. L. Iversen, B. D. Chandler, *J. Am. Chem. Soc.* **2003**, *125*, 14832.
41 K. R. Gopidas, J. K. Whitesell, M. A. Fox, *J. Am. Chem. Soc.* **2003**, *125*, 6491.
42 K. R. Gopidas, J. K. Whitesell, M. A. Fox, *J. Am. Chem. Soc.* **2003**, *125*, 14168.
43 M. Kimura, T. Shiba, M. Yamazaki, K. Hanabusa, H. Shirai, N. Kobayashi, *J. Am. Chem. Soc.* **2001**, *123*, 5636.
44 M. Kimura, Y. Saito, K. Ohta, K. Hanabusa, H. Shirai, N. Kobayashi, *J. Am. Chem. Soc.* **2002**, *124*, 5274.
45 M.-S. Choi, T. Aida, H. Luo, Y. Araki, O. Ito, *Angew. Chem., Int. Ed.* **2003**, *42*, 4060.
46 T. H. Ghaddar, J. F. Wishart, D. W. Thompson, J. K. Whitesell, M. A. Fox, *J. Am. Chem. Soc.* **2002**, *124*, 8285.
47 M. Lor, J. Thielemans, L. Viaene, M. Cotlet, J. Hofkens, T. Weil, C. Hampel, K. Müllen, J. W. Verhoeven, M. van der Auweraer, F. C. de Schryver, *J. Am. Chem. Soc.* **2002**, *124*, 9918.
48 D.-L. Jiang, T. Aida, *J. Am. Chem. Soc.* **1998**, *120*, 10895.
49 M.-S. Choi, T. Aida, T. Yamazaki, I. Yamazaki, *Angew. Chem., Int. Ed.* **2001**, *40*, 3194.
50 M.-S. Choi, T. Aida, T. Yamazaki, I. Yamazaki, *Chem. Eur. J.* **2002**, *8*, 2668.
51 M.-S. Choi, T. Yamazaki, I. Yamazaki, T. Aida, *Angew. Chem., Int. Ed.* **2004**, *43*, 150.
52 J. S. Melinger, Y. Pan, V. D. Kleiman, Z. Peng, B. L. Davis, D. McMorrow, M. Lu, *J. Am. Chem. Soc.* **2002**, *124*, 12002.
53 M. Maus, R. De, M. Lor, T. Weil, S. Mitra, U.-M. Wiesler, A. Herrmann, J. Hofkens, T. Vosch, K. Müllen, F. C. de Schryver, *J. Am. Chem. Soc.* **2001**, *123*, 7768.
54 O. P. Varnavski, J. C. Ostrowski, L. Sukhomlinova, R. J. Twieg, G. C. Bazan, T. Goodson, III, *J. Am. Chem. Soc.* **2002**, *124*, 1736.
55 M. I. Ranasinghe, Y. Wang, T. Goodson, III, *J. Am. Chem. Soc.* **2003**, *125*, 5258.
56 Y. Wang, M. I. Ranasinghe, T. Goodson, III, *J. Am. Chem. Soc.* **2003**, *125*, 9562.
57 N. D. McClenaghan, R. Passalacqua, F. Loiseau, S. Campagna, B. Verheyde, A. Hameurlaine, W. Dehaen, *J. Am. Chem. Soc.* **2003**, *125*, 5356.
58 T. Goodson, III, *Acc. Chem. Res.* **2005**, *38*, 99.
59 *Handbook of Metalloproteins*, ed. by A. Messerschmidt, R. Huber, T. Poulos, K. Wieghardt, W. Bode, M. Gygler, Wiley, **2001**.
60 M. Enomoto, T. Aida, *J. Am. Chem. Soc.* **2002**, *124*, 6099.
61 D.-L. Jiang, T. Aida, *Chem. Commun.* **1996**, 1523.
62 C. Saudan, V. Balzani, M. Gorka, S.-K. Lee, J. van Heyst, M. Maestri, P. Ceroni, V. Vicinelli, F. Vögtle, *Chem. Eur. J.* **2004**, *10*, 899.
63 C. Saudan, V. Balzani, M. Gorka, S.-K. Lee, M. Maestri, V. Vicinelli, F. Vögtle, *J. Am. Chem. Soc.* **2003**, *125*, 4424.
64 M. Uyemura, T. Aida, *Chem. Eur. J.* **2003**, *9*, 3492.
65 M. Uyemura, T. Aida, *J. Am. Chem. Soc.* **2002**, *124*, 11392.
66 P. Bhyrappa, J. K. Young, J. S. Moore, K. S. Suslick, *J. Am. Chem. Soc.* **1996**, *118*, 5708.
67 C. Valério, E. Alonso, J. Ruiz, J.-C. Blais, D. Astruc, *Angew. Chem., Int. Ed.* **1999**, *38*, 1747.
68 M.-C. Daniel, J. Ruiz, J.-C. Blais, N. Daro, D. Astruc, *Chem. Eur. J.* **2003**, *9*, 4371.
69 C. Valério, J.-L. Fillaut, J. Ruiz, J. Guittard, J.-C. Blais, D. Astruc, *J. Am. Chem. Soc.* **1997**, *119*, 2588.
70 M.-C. Daniel, J. Ruiz, S. Nlate, J.-C. Blais, D. Astruc, *J. Am. Chem. Soc.* **2003**, *125*, 2617.
71 D. de Groot, B. F. M. de Waal, J. N. H. Reek, A. P. H. J. Schenning, P. C. J. Kamer, E. W. Meijer, P. W. N. M. van Leeuwen, *J. Am. Chem. Soc.* **2001**, *123*, 8453.
72 R. van de Coevering, M. K. Robertus, J. M. K. Gebbink, G. van Koten, *Chem. Commun.* **2002**, 1636.
73 D. Astruc, F. Chardac, *Chem. Rev.* **2001**, *101*, 2991.
74 R. van Heerbeek, P. C. J. Kamer, P. W. N. M. van Leeuwen, J. N. H. Reek, *Chem. Rev.* **2002**, *102*, 3717.
75 L. J. Twyman, A. S. H. King, I. K. Martin, *Chem. Soc. Rev.* **2002**, *31*, 69.
76 D. Astruc, *Acc. Chem. Res.* **2000**, *33*, 287.
77 S. M. Cohen, S. Petoud, K. N. Raymond, *Chem. Eur. J.* **2001**, *7*, 272.
78 F. L. Derf, E. Levillain, G. Trippé, A. Gorgues, M. Sallé, R.-M. Sebastían, A.-M. Caminade, J.-P. Majoral, *Angew. Chem., Int. Ed.* **2001**, *40*, 224.
79 C. B. Gorman, J. C. Smith, *Acc. Chem. Res.* **2001**, *34*, 60.

80 C. B. Gorman, J. C. Smith, *J. Am. Chem. Soc.* **2000**, *122*, 9342.
81 T. L. Chasse, R. Sachdeva, Q. Li, Z. Li, R. J. Petrie, C. B. Gorman, *J. Am. Chem. Soc.* **2003**, *125*, 8250.
82 C. B. Gorman, J. C. Smith, M. W. Hager, B. L. Parkhurst, H. Sierzputowska-Gracz, C. A. Haney, *J. Am. Chem. Soc.* **1999**, *121*, 9958.
83 P. Weyermann, J.-P. Gisselbrecht, C. Boudon, F. Diederich, M. Gross, *Angew. Chem., Int. Ed.* **1999**, *38*, 3215.
84 P. J. Dandliker, F. Diederich, J.-P. Gisselbrecht, A. Louati, M. Gross, *Angew. Chem., Int. Ed. Engl.* **1995**, *34*, 2725.
85 P. R. Ashton, V. Balzani, M. Clemente-León, B. Colonna, L. Credi, N. Jayaraman, F. M. Raymo, J. F. Stoddart, M. Venturi, *Chem. Eur. J.* **2002**, *8*, 673.
86 D. L. Stone, D. K. Smith, P. T. McGrail, *J. Am. Chem. Soc.* **2002**, *124*, 856.
87 S. A. Vinogradov, D. F. Wilson, *Chem. Eur. J.* **2000**, *6*, 2456.
88 K. W. Pollak, J. W. Leon, J. M. J. Fréchet, M. Maskus, H. D. Abruña, *Chem. Mater.* **1998**, *10*, 30.
89 R. Sadamoto, N. Tomioka, T. Aida, *J. Am. Chem. Soc.* **1996**, *118*, 3978.
90 D.-L. Jiang, C.-K. Choi, K. Honda, W.-S. Li, T. Yuzawa, T. Aida, *J. Am. Chem. Soc.* **2004**, *126*, 12084.
91 S. A. Vinogradov, L.-W. Lo, D. F. Wilson, *Chem. Eur. J.* **1999**, *5*, 1338.
92 F. Vögtle, M. Plevoets, M. Nieger, G. C. Azzellini, A. Credi, L. de Cola, V. de Marchis, M. Venturi, V. Balzani, *J. Am. Chem. Soc.* **1999**, *121*, 6290.
93 R. Kunieda, M. Fujitsuka, O. Ito, M. Ito, Y. Murata, K. Komatsu, *J. Phys. Chem. B* **2002**, *106*, 7193.
94 S. Hecht, N. Vladimirov, J. M. J. Fréchet, *J. Am. Chem. Soc.* **2001**, *123*, 18.
95 T. Sato, D.-L. Jiang, T. Aida, *J. Am. Chem. Soc.* **1999**, *121*, 10658.
96 F. S. Precup-Glaga, J. C. Garcia-Martinez, A. P. H. J. Schenning, E. W. Meijer, *J. Am. Chem. Soc.* **2003**, *125*, 12953.
97 W.-D. Jang, N. Nishiyama, G.-D. Zhang, A. Harada, D.-L. Jiang, S. Kawauchi, Y. Morimoto, M. Kikuchi, H. Koyama, T. Aida, K. Kataoka, *Angew. Chem., Int. Ed.* **2005**, *44*, 419.
98 P. Ceroni, F. Paolucci, C. Paradisi, A. Juris, S. Roffia, S. Serroni, S. Campagna, A. J. Bard, *J. Am. Chem. Soc.* **1998**, *120*, 5480.
99 M. Marcaccio, F. Paolucci, C. Paradisi, S. Roffia, C. Fontanesi, L. J. Yellowlees, S. Serroni, S. Campagna, G. Denti, V. Balzani, *J. Am. Chem. Soc.* **1999**, *121*, 10081.
100 K. Yamamoto, M. Higuchi, A. Kimoto, T. Imaoka, K. Masachika, *Bull. Chem. Soc. Jpn.* **2005**, *78*, 349.
101 M. Higuchi, S. Shiki, K. Ariga, K. Yamamoto, *J. Am. Chem. Soc.* **2001**, *123*, 4414.
102 M. Higuchi, K. Yamamoto, *Bull. Chem. Soc. Jpn.* **2004**, *77*, 853.
103 K. Yamamoto, M. Higuchi, S. Shiki, M. Tsuruta, H. Chiba, *Nature* **2002**, *415*, 509.
104 M. Higuchi, M. Tsuruta, H. Chiba, S. Shiki, K. Yamamoto, *J. Am. Chem. Soc.* **2003**, *125*, 9988.
105 N. Satoh, J.-S. Cho, M. Higuchi, K. Yamamoto, *J. Am. Chem. Soc.* **2003**, *125*, 8104.
106 T. Imaoka, H. Horiguchi, K. Yamamoto, *J. Am. Chem. Soc.* **2003**, *125*, 340.
107 O. Enoki, T. Imaoka, K. Yamamoto, *Org. Lett.* **2003**, *5*, 2547.
108 R. Nakajima, M. Tsuruta, M. Higuchi, K. Yamamoto, *J. Am. Chem. Soc.* **2004**, *126*, 1630.
109 C. L. Jackson, H. D. Chanzy, F. P. Booy, B. J. Drake, D. A. Tomalia, B. J. Bauer, E. J. Amis, *Macromolecules* **1998**, *31*, 6259.
110 P. W. Morgan, S. L. Kwolek, T. C. Pletcher, *Macromolecules* **1987**, *20*, 729.
111 R. Tanaka, T. Imaoka, K. Yamamoto, *J. Photopolym. Sci. Technol.* **2004**, *17*, 323.
112 E. M. Harth, S. Hecht, B. Helms, E. E. Malmstrom, J. M. J. Fréchet, C. J. Hawker, *J. Am. Chem. Soc.* **2002**, *124*, 3926.
113 J. H. Burroughes, D. D. C. Bradely, A. R. Brown, R. N. Marks, K. Mackay, R. H. Friend, P. L. Burns, A. B. Holmes, *Nature* **1990**, *347*, 539.
114 R. H. Friend, R. W. Gymer, A. B. Holmes, J. H. Burroughes, R. N. Marks, C. Taliani, D. D. C. Bradely, D. A. Dos Santos, J. L. Bredas, M. Logdlund, W. R. Salaneck, *Nature* **1999**, *397*, 121.
115 A. Kimoto, J.-S. Cho, M. Higuchi, K. Yamamoto, *Macromolecules* **2004**, *37*, 5531.
116 H. Arakawa, M. Aresta, J. N. Armor, M. A. Barteau, E. J. Beckman, A. T. Bell, J. E. Bercaw, C. Creutz, E. Dinjus, D. A. Dixon, K. Domen, D. L. DuBois, J. Eckert, E. Fujita, D. H. Gibson, W. A. Goddard, III, D. W. Goodman, J. Keller, G. J. Kubas, H. H. Kung, J. E. Lyons, L. E. Manzer, T. J. Marks, K. Morokuma, K. M. Nicholas, R. Periana, L. Que, J. Rostrup-Nielson, W. M. H. Sachtler, L. D. Schmidt, A. Sen, G. A. Somorjai, P. C. Stair, B. R. Stults, W. Tumas, *Chem. Rev.* **2001**, *101*, 953.
117 D. Behar, T. Dhanasekaran, P. Neta, C. M. Hosten, D. Ejeh, P. Hambright, E. Fujita, *J. Phys. Chem. A* **1998**, *102*, 2870.
118 E. Fujita, C. Creutz, N. Sutin, D. J. Szalda, *J. Am. Chem. Soc.* **1991**, *113*, 343.
119 I. Bhugun, D. Lexa, J.-M. Savéant, *J. Phys. Chem.* **1996**, *100*, 19981.
120 T. Imaoka, R. Tanaka, S. Arimoto, M. Sakai, M. Fujii, K. Yamamoto, *J. Am. Chem. Soc.* **2005**, *127*, 13896.
121 H.-Z. Yu, J. S. Baskin, B. Steiger, F. C. Anson, A. H. Zewail, *J. Am. Chem. Soc.* **1999**, *121*, 484.
122 X. Liu, E. C. Theil, *Acc. Chem. Res.* **2005**, *38*, 167.
123 A. Ilari, S. Stefanini, E. Chiancone, D. Tsernoglou, *Nat. Struct. Biol.* **2000**, *7*, 38.
124 M. J. Frisch, G. W. Trucks, H. B. Schlegel, G. E. Scuseria, M. A. Robb, J. R. Cheeseman, J. A. Montgomery, Jr., T. Vreven, K. N. Kudin, J. C. Burant, J. M. Millam, S. S. Iyengar, J. Tomasi, V. Barone, B. Mennucci, M. Cossi, G. Scalmani, N. Rega, G. A. Petersson, H. Nakatsuji, M. Hada, M. Ehara, K. Toyota, R. Fukuda, J. Hasegawa, M. Ishida, T. Nakajima, Y. Honda, O. Kitao, H. Nakai, M. Klene, X. Li, J. E. Knox, H. P. Hratchian, J. B. Cross, C. Adamo, J. Jaramillo, R. Gomperts, R. E. Stratmann, O. Yazyev, A. J. Austin, R. Cammi, C. Pomelli, J. W. Ochterski, P. Y. Ayala, K. Morokuma, G. A. Voth, P. Salvador, J. J. Dannenberg, V. G. Zakrzewski, S. Dapprich, A. D. Daniels, M. C. Strain, O. Farkas, D. K. Malick, A. D. Rabuck, K. Raghavachari, J. B. Foresman, J. V. Ortiz, Q. Cui, A. G. Baboul, S. Clifford, J. Cioslowski, B. B. Stefanov, G. Liu, A. Liashenko, P. Piskorz, I. Komaromi, R. L. Martin, D. J. Fox, T. Keith, M. A. Al-Laham, C. Y. Peng, A. Nanayakkara, M. Challacombe, P. M. W. Gill, B. Johnson, W. Chen, M. W. Wong, C. Gonzalez, J. A. Pople, *Gaussian 03, Revision C.02*, Gaussian, Inc., Wallingford CT, **2004**.

Kimihisa Yamamoto received B.S., M.S., and Ph.D. degrees from Waseda University in Polymer Chemistry in 1985, 1987, and 1990, respectively. He was a Research Associate and Assistant Professor of Waseda University from 1989 to 1991 and from 1992 to 1993, respectively. He was Associate Professor of Waseda University from 1993 to 1996. He is now a professor of Department of Chemistry in Keio University from 1997. He has received the Award for the Young Chemist from Chemical Society of Japan in 1996 and the JSPS Wiley Award in 2005 from the Society of Polymer Science, Japan. He promoted research projects as a researcher of Japan Research Development Corporation for PRESTO project from 1992 to 1994; he was a project leader in Kanagawa Academy of Science and Technology (KAST) from 2002 to 2004, and a leader for the CREST project in Japan Science and Technology Agency (JST) from 2003 to present. He is engaged in developing supra-metallomolecules. He is a member of the Japan Chemical Society.

Takane Imaoka graduated from Keio University in 2000 and received his Ph.D. degree from the same university in 2005 under the supervision of Professor Kimihisa Yamamoto. He received the JSPS Research Fellowships for Young Scientists during 2002–2004. He is now a Research Associate at Keio University, Department of Chemistry from 2004. His current research interests focus on the electron-transfer chemistry in dendritic macromolecules for molecular electronics and catalysis.